Proceedings of the Estonian Academy of Sciences,
2018, **67**, 1, 61–72
https://doi.org/10.3176/proc.2018.1.03
Available online at www.eap.ee/proceedings

CONTROL
THEORY

Newton observer for a nonlinear flux-controlled AMB system

Arkadiusz Mystkowski[a], Ülle Kotta[b], and Vadim Kaparin[b]*

[a] Department of Automatic Control and Robotics, Białystok University of Technology, Wiejska 45A, 15-351 Białystok, Poland; a.mystkowski@pb.edu.pl
[b] Department of Software Science, School of Information Technologies, Tallinn University of Technology, Akadeemia tee 21, 12618 Tallinn, Estonia; kotta@cc.ioc.ee

Received 10 April 2017, accepted 13 July 2017, available online 31 January 2018

Abstract. The paper focuses on the adaptation of the Newton observer for the estimation of the magnetic flux in the feedback control of a nonlinear active magnetic bearing (AMB) system. The Newton observer is constructed for the exact discrete-time model of the AMB system and is presented in a detailed and simple algorithm ready for implementation. The observer is combined with three controllers, and the effectiveness of the observer-based control scheme is verified via numerical simulations.

Key words: active magnetic bearing, Newton observer.

1. INTRODUCTION

Active magnetic bearing (AMB) applications are frequently controlled by the feedback, depending on the magnetic flux. The flux measurement requires additional expensive sensors to be integrated mechanically into the AMB poles [10]. Therefore, the so-called sensorless control has emerged, where traditional sensors are replaced by a signal from a dynamic estimator. Nowadays, the 'self-sensing' magnetic bearing technology is employed in many commercial applications, see for instance [24,11]. It has been found that the position and speed signals may be used to estimate the electrical information as the magnetic flux [20].

The purpose of this paper is to address the problem of state estimation of a nonlinear flux-controlled AMB system operated in the low- or zero-bias mode. A number of papers address the application of nonlinear observers for AMB systems, but the majority of AMB flux estimation methods are developed for the *bias control* and are based on the rotor position or measurements of the output current [2,9]. The high-gain observer is suggested in [5] for the voltage-controlled 3-pole AMB system. This observer is incorporated in the AMB system in the *current-controlled mode* to use the information of input voltages and output coil currents for the estimation of the rotor position. The authors have additionally assumed the magnetic field to be linear in the sense that the magnetic flux density is proportional to the magnetic field intensity. However, the saturation problems, which always exist in a current/voltage-controlled AMB system, were not addressed. Note that, unlike [5], in this work we consider the *zero-bias flux-controlled* AMB system, which contains the class of nonlinearity (dead zone near the origin) and control input voltage limit inappropriate for the application of the high-gain observer. The disturbance observer-based control of AMB was addressed in [18].

* Corresponding author, vkaparin@cc.ioc.ee

The zero- or low-bias control has many advantages in comparison with the bias control [22,23], including the reduction of power losses, low bearing stiffness, and low noise in the position measurements. In [20] the controller for AMB in the low-bias control mode is presented, combined with the nonlinear circle-criterion observer, developed in [1], which makes use of the bounds on the slope of system nonlinearities. The circle criterion states that the feedback interconnection of such sector nonlinearity with a strictly positive real linear block is asymptotically stable. However, the nonlinearity of the controllers used in this paper makes this method inappropriate for the solution of the stated problem. In [19] the sliding-mode observers were incorporated in the zero-bias flux feedback, the model of which differs from the one considered in this paper. Although the sliding-mode observers are, in principle, appropriate for the model considered in this paper, their application is beyond the topic of this research.

The Newton observer [14] is known to be structurally robust and has been reported to yield good results, see for example [3,6,13]. It yields an asymptotic observer (i.e. an observer whose error converges to zero as time tends to infinity) for a large class of discrete-time nonlinear systems. The observer relies on an analytical expression for the exact discrete-time model of the continuous-time system. Although this assumption may in general be a shortcoming, it does not limit the applicability in our case when the rather simple exact discrete-time model exists for the AMB. Moreover, the Newton observer does not require any restrictive assumptions to be satisfied by the system equations, and its construction does not involve any state transformations (into a special canonical form), implying less need in computational capacity.

The basic idea of the Newton observer is to view the state estimation problem as one of solving a sequence of nonlinear inversion problems, each described by a set of nonlinear equations. The intention then is to iterate each subproblem long enough so that the state transition map applied to the solution of the kth problem is a good initial guess for the $(k+1)$st problem. The Newton observer may be understood as a quasilocal exponential observer, whose iterations converge to the solution of the set of nonlinear equations only if the initial guess is close enough to the solution. To relax this restriction, one may enlarge the convergence region by changing the step size at each iteration as suggested, for example, in [4]. In particular, global convergence is guaranteed when one utilizes, for instance, a line-search scheme to find the suitable step size. Note, however, that here we do not need to relax this restriction because the physical structure of the AMB system does not allow choosing the initial guess too far from the solution.

The paper is organized as follows. Section 2 describes the AMB system and develops its exact discrete-time model. The detailed construction of the Newton observer for the exact discrete-time model as well as the algorithm of the observer implementation are given in Section 3. Section 4 presents the simulation results, verifying the effectiveness of the Newton observer in the feedback control of the AMB system. Section 5 presents the concluding remarks.

2. CONTROL SYSTEM AND ITS EXACT DISCRETE-TIME MODEL

Consider a continuous-time nonlinear plant, described by the differential equations

$$\dot{x} = f(x) + g(x)u, \quad y = h(x), \tag{1}$$

where the state $x \in \mathbb{R}^n$, the control input $u \in \mathbb{R}$, the output $y \in \mathbb{R}$, and f, g, h are smooth functions.

The exact step-invariant discrete-time model of the continuous-time system (1) is defined as the one whose response to a step input (i.e. the type of input usually available under digital control) $u(kT+t) = u(kT), 0 \le t < T$, is identical to that of the continuous-time system at discrete instants of time. The derivation of a discrete-time model is based on the representation of the solution of Eq. (1) in terms of the formal Lie exponential series at sampling instant $kT+T$ (see [8,12])

$$x(kT+T) = \sum_{r\ge 0} \frac{T^r}{r!} L^r_{f+gu(kT)} x \Big|_{x(kT)} =: F(x(kT), u(kT)), \quad y(kT) = h(x(kT)), \tag{2}$$

where $L^r_{f+gu(kT)}$ denotes the rth Lie derivative along $f + gu(kT)$.

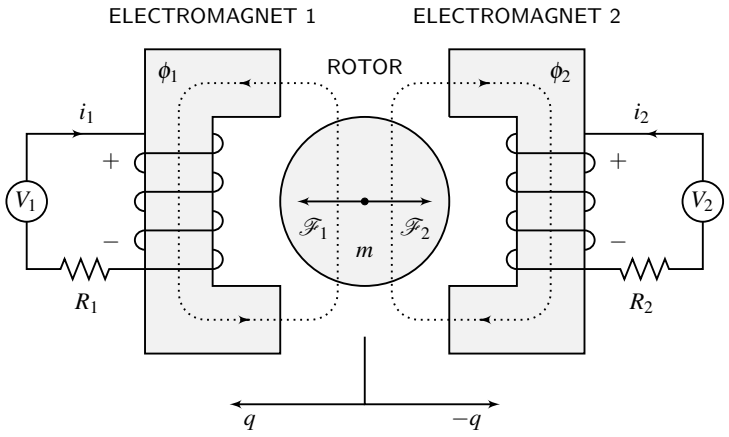

Fig. 1. Scheme of a 1-DOF AMB.

In this paper we consider a simplified one-degree-of-freedom (1-DOF) AMB model that consists of two opposite and presumably identical electromagnetic actuators (electromagnets) with resistances R_1, R_2 and currents i_1, i_2, respectively (see Fig. 1). These electromagnets generate fluxes ϕ_1, ϕ_2 and further the attractive forces $\mathscr{F}_1$, $\mathscr{F}_2$, acting on the rotor. In order to control the position q of the rotor mass m to the stable point $q = 0$, the voltage inputs of the electromagnets V_1 and V_2 are used. The 1-DOF AMB system is limited to a rigid rotor mass. In order to make the system simpler, the observer-based flux control is considered only in one control axis. Thus, in our case, the rotor dynamics are not addressed.

The dynamics of the simplified 1-DOF AMB model may be described in terms of normalized state and control variables by the following nonlinear state equations:

$$\dot{x}_1 = x_2, \quad \dot{x}_2 = \varepsilon x_3 + x_3 |x_3|, \quad \dot{x}_3 = u, \tag{3}$$

where x_1, x_2, and x_3 indirectly relate to the position [m] of the rotor mass, velocity [m/s] and electromagnetic flux [Wb], respectively (see [21] for details). Moreover, $\varepsilon = 2\Phi_0/\Phi_{\text{sat}} \geq 0$, where Φ_0 and Φ_{sat} stand for the bias and saturation fluxes, respectively. For the Newton observer design we assume that the output $y = x_1$. In (3), $f = \begin{bmatrix} x_2 & \varepsilon x_3 + x_3 |x_3| & 0 \end{bmatrix}^{\mathsf{T}}$, being smooth under the assumption $x_3 \neq 0$, and $g = \begin{bmatrix} 0 & 0 & 1 \end{bmatrix}^{\mathsf{T}}$. Based on (2), one obtains the sampled-data model of system (3) as

$$\begin{aligned}
x_1^{[1]} &= x_1 + Tx_2 + \frac{T^2}{2}(\varepsilon x_3 + x_3|x_3|) + \frac{T^3}{6}u(\varepsilon + 2\operatorname{sgn}(x_3)x_3) + \frac{T^4}{12}u^2\operatorname{sgn}(x_3), \\
x_2^{[1]} &= x_2 + T(\varepsilon x_3 + x_3|x_3|) + \frac{T^2}{2}u(\varepsilon + 2\operatorname{sgn}(x_3)x_3) + \frac{T^3}{3}u^2\operatorname{sgn}(x_3), \qquad (4a) \\
x_3^{[1]} &= x_3 + uT, \\
y &= x_1, \qquad (4b)
\end{aligned}$$

where we use the abridged notation, i.e. $x_i^{[1]} := x_i(kT+T)$, $x_i := x_i(kT)$, for $i = 1,2,3$, and $u := u(kT)$, $y := y(kT)$. Note that (4) is the exact sampled-data model, since all terms of the sum in (2) for $r \geq 5$ are equal to zero. Note also that in the development of (4) we assumed that $\frac{\mathrm{d}}{\mathrm{d}x_3}|x_3| = \operatorname{sgn}(x_3)$ and $\frac{\mathrm{d}}{\mathrm{d}x_3}\operatorname{sgn}(x_3) = 0$, which is not valid at the point $x_3 = 0$.

3. NEWTON OBSERVER

Hereinafter $\xi^{[j]}$ denotes $\xi(kT+jT)$ for $j \in \mathbb{Z}$. Moreover, we denote $x := \begin{bmatrix} x_1 & x_2 & x_3 \end{bmatrix}^\mathsf{T}$ and $x^{[j]} := \begin{bmatrix} x_1^{[j]} & x_2^{[j]} & x_3^{[j]} \end{bmatrix}^\mathsf{T}$. Here we adopt the Newton observer [14] for system (4). We introduce the following notations: $Y_{[k-2,k]} := \begin{bmatrix} y^{[-2]} & y^{[-1]} & y \end{bmatrix}^\mathsf{T}$, $U_{[k-2,k-1]} := \begin{bmatrix} u^{[-2]} & u^{[-1]} \end{bmatrix}^\mathsf{T}$, where $Y_{[k-2,k]}$ is a vector (buffer) of the successive system measured outputs starting with the output at the time instant $kT-2T$, and $U_{[k-2,k-1]}$ is a vector of the successive system measured inputs starting with the input at the time instant $kT-2T$. Moreover, we denote $H\left(x^{[-2]}, U_{[k-2,k-1]}\right) := \begin{bmatrix} h_1 & h_2 & h_3 \end{bmatrix}^\mathsf{T}$, where

$$
\begin{aligned}
h_1 :=& h\left(x^{[-2]}\right) = x_1^{[-2]},\\
h_2 :=& h\left(F\left(x^{[-2]}, u^{[-2]}\right)\right) = x_1^{[-2]} + Tx_2^{[-2]} + \frac{T^2}{2}\left(\varepsilon x_3^{[-2]} + x_3^{[-2]}\left|x_3^{[-2]}\right|\right)\\
&+ \frac{T^3}{6}u^{[-2]}\left(\varepsilon + 2\operatorname{sgn}(x_3^{[-2]})x_3^{[-2]}\right) + \frac{T^4}{12}\left(u^{[-2]}\right)^2\operatorname{sgn}(x_3^{[-2]}),\\
h_3 :=& h\left(F\left(F\left(x^{[-2]}, u^{[-2]}\right), u^{[-1]}\right)\right) = \frac{1}{12}\Big(5T^4\operatorname{sgn}\left(x_3^{[-2]}\right)\left(u^{[-2]}\right)^2 + T^4\operatorname{sgn}\left(Tu^{[-2]} + x_3^{[-2]}\right)\left(u^{[-1]}\right)^2\\
&+ 2T^3u^{[-2]}\left(7\varepsilon + 3\left|Tu^{[-2]} + x_3^{[-2]}\right| + 2T\operatorname{sgn}\left(Tu^{[-2]} + x_3^{[-2]}\right)u^{[-1]} + 8\operatorname{sgn}\left(x_3^{[-2]}\right)x_3^{[-2]}\right)\\
&+ 2T^3u^{[-1]}\left(\varepsilon + 2\operatorname{sgn}\left(Tu^{[-2]} + x_3^{[-2]}\right)x_3^{[-2]}\right) + 6\Big(2x_1^{[-2]} + T\Big(4x_2^{[-2]} + T\Big(4\varepsilon + 3\left|x_3^{[-2]}\right| + \left|Tu^{[-2]} + x_3^{[-2]}\right|\Big)x_3^{[-2]}\Big)\Big)\Big).
\end{aligned}
$$

The vector H displays the same outputs as those given in $Y_{[k-2,k]}$ but generated from the retarded state $x^{[-2]} := x(kT-2T)$ using multiple compositions of the system forward dynamics (4a) and the system output map (4b).

The construction of the Newton observer is based on the solution of the set of nonlinear equations

$$
Y_{[k-2,k]} - H\left(x^{[-2]}, U_{[k-2,k-1]}\right) = 0 \tag{5}
$$

with respect to $x^{[-2]}$. The approach requires the iterative solution of (5) for each time interval. The Newton observer applies Newton's method to find the solution. Equations (5) are defined by an observability mapping (one set of equations for each sampling period). Observe that for simplicity (to avoid application of pseudo-inverse) we assumed that in (5) the set of equations to be solved is square. That is, since the number of states to be estimated is three we have taken three equations*.

Once the solution of (5) is found, i.e. the retarded state $x^{[-2]}$ is reconstructed, the current value of the state x can be recovered by forwarding $x^{[-2]}$ twice using multiple composition of (4a). In particular,

$$
x = F\left(F\left(x^{[-2]}, u^{[-2]}\right), u^{[-1]}\right).
$$

To resume, the Newton observer is composed of an iterative solution of Eq. (5) and shift-forwarding (extrapolating) the retarded state estimate to the current state estimate.

Below a detailed algorithm is given to find the state estimates for this specific case – three states to be estimated, one control variable, three equations (with buffer two). Note that the Jacobian

$$
\left[\partial H/\partial w_i^{[k]}\left(w_i^{[k]}, U_{[k-2,k-1]}\right)\right]^{-1}
$$

can be computed symbolically.

* In the case when the number of equations exceeds the number of states, the inverse in (6) should be replaced by a pseudoinverse.

Algorithm

Input: d, $k_{\max}$. Output: state estimates = { }.

Step 1. Set $w_0^{[0]}$.

Step 2. Set $k = 0$.

Step 3. Set $i = 0$.

Step 4. Compute

$$w_{i+1}^{[k]} = w_i^{[k]} + \Upsilon_i^{[k]}, \tag{6}$$

where $\Upsilon_i^{[k]} := \left[\frac{\partial H}{\partial w_i^{[k]}}\left(w_i^{[k]}, U_{[k-2,k-1]}\right)\right]^{-1}\left(Y_{[k-2,k]} - H\left(w_i^{[k]}, U_{[k-2,k-1]}\right)\right)$.

Step 5. Set $i := i+1$.

Step 6. If $i \leq d-1$ (where d is a design parameter) then go to Step 4.

Step 7. Set $w_0^{[k+1]} = F\left(w_d^{[k]}, u^{[k-2]}\right)$.

Step 8. The estimate is $\hat{x}^{[k]} = F\left(w_0^{[k+1]}, u^{[k-1]}\right)$. Add $\hat{x}^{[k]}$ into the ordered set of estimates.

Step 9. Set $k := k+1$.

Step 10. If $k \leq k_{\max}$ then go to Step 3.

Step 11. Return the state estimates.

Remarks

1. The design parameter $k_{\max}$ defines the number of time instances for which we want to estimate the state variables. Since the Newton observer is an asymptotic observer, small values of $k_{\max}$ can lead to insufficiently accurate estimates.

The design parameter d defines the number of iterations in Newton's method. It is demonstrated in [7] that increasing the number of iterations until it is big enough has a small effect upon observer performance. Moreover, in case of measurement noise, increasing d may even have an undesirable effect. In our simulations we took $d = 10$. This value was obtained as a result of the trial and error process performed during simulations.

2. In case of measurement noise, it is desirable, as demonstrated in [7], to introduce the third design parameter α, i.e. to replace Eq. (6) by $w_{i+1}^{[k]} = w_i^{[k]} + \alpha\Upsilon_i^{[k]}$, $0 < \alpha < 1$. By setting $\alpha = 1$, the fastest observer but the one with poor measurement noise rejection properties is achieved. Decreasing α will improve the noise rejection ability of the observer.

3. Note that in the implementation we compute the expression $\Upsilon_i^{[k]}$ in (6) symbolically.

4. The sampling rate in (4) cannot be taken too small; for fast sampling rates the observability map (5) (to be inverted) may become ill-conditioned. This may also happen when the system is weakly observable.

5. The vector $w_0^{[0]}$ contains initial estimates of the states at the time instant $kT - 2T$. For the Newton observer to converge, $w_0^{[0]}$ has to be close enough to the actual state $x^{[-2]}$ (for the detailed discussion on the convergence of the Newton observer we refer the reader to [14]). If the discrete Newton's method does not converge, one may use a quasi-Newton observer with a varying step size $w_{i+1}^{[k]} = w_i^{[k]} + \lambda_{i,k}\Upsilon_i^{[k]}$ or one may apply a computationally more expensive continuous method [4]. The latter method is not described here since we did not face any convergence problems.

3.1. Reduced-order Newton observer

Note that the variable x_1 is available from measurements and $x_2 = \dot{x}_1$ can be estimated using a low-pass filter. Therefore, the reduced-order Newton observer can be applied to estimate the variable x_3 only.

As a low-pass filter for x_2 one may use $(\mathrm{d}T_s/\mathrm{d}t)\,x_2 + x_2 = (\mathrm{d}/\mathrm{d}t)\,x_1$, where T_s is a time constant of the filter and the derivatives are approximated by the backward difference $(x(kT) - x((k-1)T))/T$.

Next, in the construction of the reduced-order Newton observer we use the notations

$$\bar{Y}_{[k,k]} := y,$$
$$\bar{H}\left(x_3^{[-1]}, \hat{x}_1^{[-1]}, \hat{x}_2^{[-1]}, u^{[-1]}\right) := h\left(F\left(x_3^{[-1]}, \hat{x}_1^{[-1]}, \hat{x}_2^{[-1]}, u^{[-1]}\right)\right) = \hat{x}_1^{[-1]} + T\hat{x}_2^{[-1]}$$
$$+ \frac{T^2}{2}\left(\varepsilon x_3^{[-1]} + x_3^{[-1]}\left|x_3^{[-1]}\right|\right) + \frac{T^3}{6}u^{[-1]}\left(\varepsilon + 2\mathrm{sgn}(x_3^{[-1]})x_3^{[-1]}\right) + \frac{T^4}{12}\left(u^{[-1]}\right)^2\mathrm{sgn}(x_3^{[-1]}),$$

where $\hat{x}_1^{[-1]}$ stands for the measurement of $x_1^{[-1]}$ and $\hat{x}_2^{[-1]}$ is the estimate of $x_2^{[-1]}$.

The construction of the reduced-order Newton observer is based on the solution of the nonlinear equation

$$\bar{Y}_{[k,k]} - \bar{H}\left(x_3^{[-1]}, \hat{x}_1^{[-1]}, \hat{x}_2^{[-1]}, u^{[-1]}\right) = 0 \tag{7}$$

for $x_3^{[-1]}$. Once the solution of (7) is found, i.e. the retarded state $x_3^{[-1]}$ is reconstructed, the current estimate of the state x_3 can be recovered by forwarding $x_3^{[-1]}$ once using the composition of (4a).

In the Algorithm only Steps 4, 7, and 8 require slight notational modifications. At Step 4

$$\Upsilon_i^{[k]} := \left[\frac{\partial \bar{H}}{\partial w_i^{[k]}}\left(w_i^{[k]}, \hat{x}_1^{[k-1]}, \hat{x}_2^{[k-1]}, u^{[k-1]}\right)\right]^{-1}\left(Y_{[k,k]} - \bar{H}\left(w_i^{[k]}, \hat{x}_1^{[k-1]}, \hat{x}_2^{[k-1]}, u^{[k-1]}\right)\right).$$

Moreover, Steps 7 and 8 merge into one step, where

$$\hat{x}_3^{[k]} = F\left(w_d^{[k]}, \hat{x}_1^{[k-1]}, \hat{x}_2^{[k-1]}, u^{[k-1]}\right).$$

4. SIMULATION RESULTS

The AMB nonlinear 1-DOF system is described by state equations (3). The problem is to stabilize the rotor mass at $x = \begin{bmatrix}0 & 0 & 1e-9\end{bmatrix}^{\mathsf{T}}$ using the measurements of the rotor position x_1, while the magnetic flux x_3 and the rotor velocity x_2 are not measurable and therefore not directly available for feedback.

For the AMB model, the discrete form of the control law with the estimates of the rotor velocity $\hat{x}_2$ and flux $\hat{x}_3$ is given by $u(k) = \alpha\,(x_1(k), \hat{x}_2(k), \hat{x}_3(k))$.

The results are presented for three controllers, developed in [16] to stabilize the rotor mass,

$$u_1 = -3x_1^2\hat{x}_3 - 2\hat{x}_2|\hat{x}_3| - 3x_1\hat{x}_2\hat{x}_3 - \hat{x}_3 + u_0, \tag{8a}$$
$$u_2 = \frac{1}{2}\left(3x_1^2 + 2\hat{x}_2\hat{x}_3|\hat{x}_3| + 3x_1\hat{x}_2 - \hat{x}_3\right) + u_0, \tag{8b}$$
$$u_3 = -\hat{x}_2|\hat{x}_3| - \hat{x}_3 - x_1\hat{x}_2\hat{x}_3 + u_0, \tag{8c}$$

where $u_0 = -k_1x_1 - k_2x_2$ with the gains $k_1 = 0.92$ and $k_2 = 9.94$, optimized and evaluated in the previous work [17]. These gains are kept constant for all simulations.

Table 1. Parameters of the simulation and AMB system

Parameter	Symbol	Unit	Value
Sampling time	T	s	0.001
Maximum number of samples	$k_{\max}$		1000
Design parameter	d		100
Options of initial value for rotor position	$x_1(0)$	m	$\{0, 0.001, 0.01\}$
Initial value for rotor velocity	$x_2(0)$	m/s	0
Initial value for magnetic flux	$x_3(0)$	Wb	$1e-9$
Options of initial value for controller output	$u(0)$	V	$\{-50, -100, -150\}$
Simulation time	$t_{\max}$	s	10
Saturation of controller output	u_{sat}	V	± 150

This section verifies via numerical simulations whether the Newton observer, adapted to system (3) as described in Section 3, can be efficiently combined with the controllers (8) for the solution of the aforementioned stability problem. All simulations are performed for the AMB control system with control voltage saturation. The parameters of the simulation and AMB system are collected in Table 1. The dynamics of the AMB system together with its exact discrete-time model (4) and the Newton observer algorithm are implemented and simulated by using the Matlab software with fixed sampling time T. Convergence of the proposed observer is evaluated by comparing its outputs, the state estimates, with the known actual states of the closed-loop AMB system under three controllers described by (8). First, we compare the outputs of the Newton observer with the known states of the flux-controlled AMB system. Note that the Newton observer (6) is incorporated into the implementation of the controllers (8). Then, estimation quality of the Newton observer-based state feedback and stability of the observer-based closed-loop system are evaluated.

Figures 2 and 3 demonstrate the convergence of the full-order Newton observer for the estimation of the state vector $x = [x_1 \ x_2 \ x_3]^{\mathsf{T}}$ with controller (8a). One may observe that the error between the estimate and the actual value converges to zero in time, not exceeding 0.05 s for all three states. The first step of the Newton observer algorithm needs to provide an initial guess for the vector $w_0(kT) = [x_1(kT-2T) \ x_2(kT-2T) \ x_3(kT-2T)]^{\mathsf{T}}$. The proper choice of the initial values for this vector components is essential. In our simulation the initial value of the rotor position $x_1(0)$ has three options $\{0, 0.001, 0.01\}$ while the initial rotor speed $x_2(0) = 0$ and the magnetic flux $x_3(0) = 1e-9$.

Remark 6. Note that the choice of small initial values for the observer is conditioned by the structural limitations of the physical AMB system, where the rotor displacement is very small due to the quite small air gap, which ensures high displacement stiffness.

One can observe from Figs 2 and 3 that the employed observer-based controller is robust to different initial values of the rotor position $x_1(0)$. Figure 3 presents comparison of the true states and their estimate for the initial condition $x_1(k-2) = 0.01$, when the convergence error is the greatest. In all cases the convergence of the observer is lost only for the first steps of the simulation. This situation is also shown in Fig. 2c, where the estimation errors are given for the first 0.5 s of the simulation time.

Figure 4 presents the responses of the observer-based closed-loop system to different initial values of the controller output $u(0)$, i.e. $\{-50, -100, -150\}$. These responses are compared with the state feedback trajectories without the observer. The Newton observer converges in all three cases. However, the stability of the observer-based feedback-controlled system strongly depends on the chosen initial values, i.e. (due to the natural behaviour of the flux-controlled AMB system operating in zero-bias mode) a larger initial value of u gives a more stable closed-loop system. Note, however, that the initial value of u should not exceed the value of saturation u_{sat}.

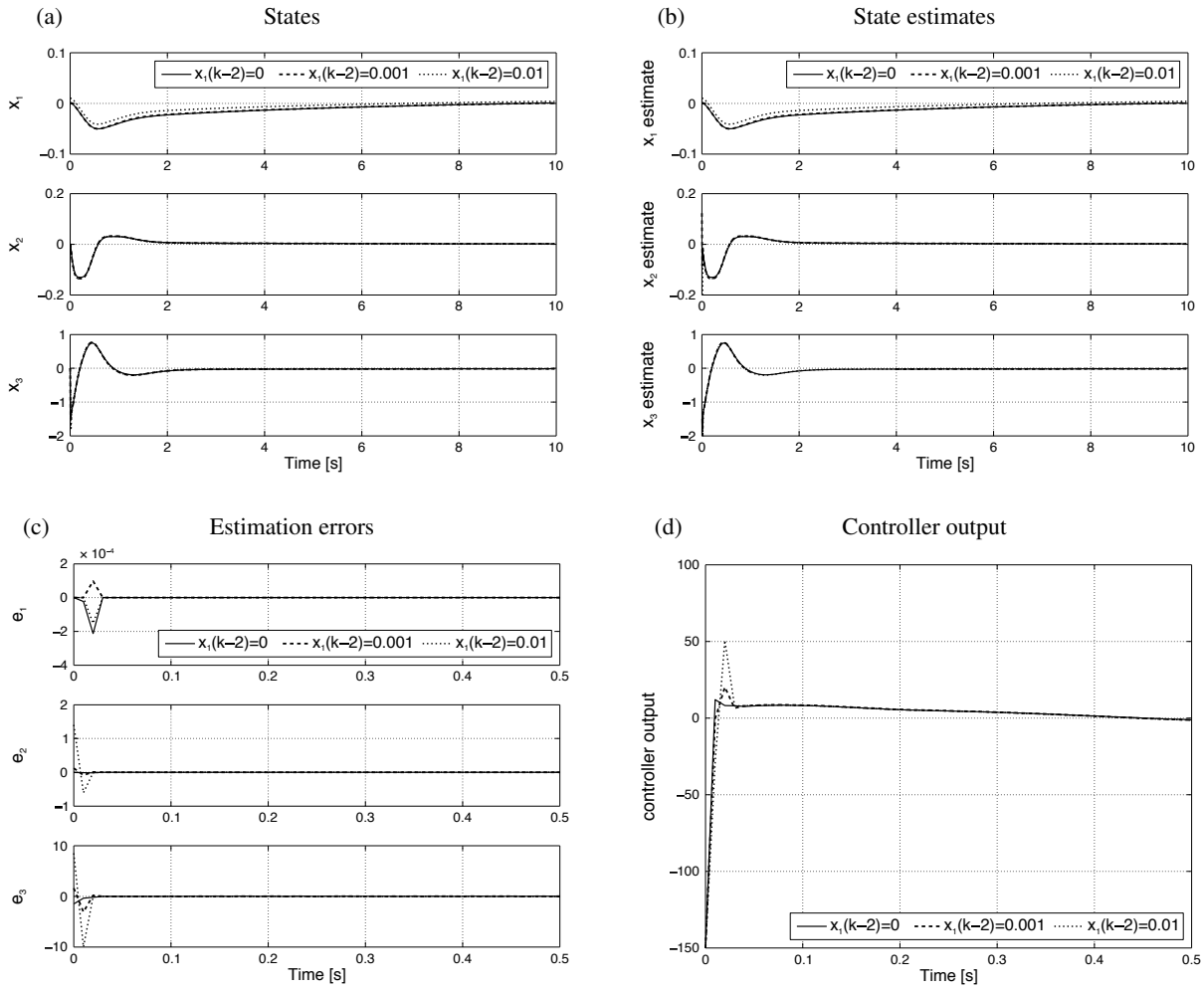

Fig. 2. Observer-based feedback responses to changes of the initial values of the rotor position with the control law (8a).

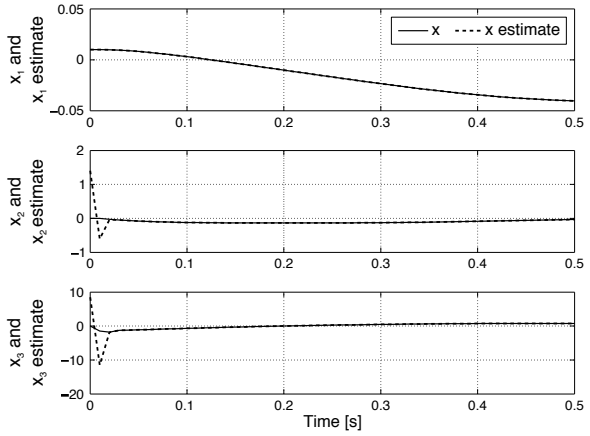

Fig. 3. Comparison of the true states and state estimates for the initial condition $x_1(k-2) = 0.01$ with the control law (8a).

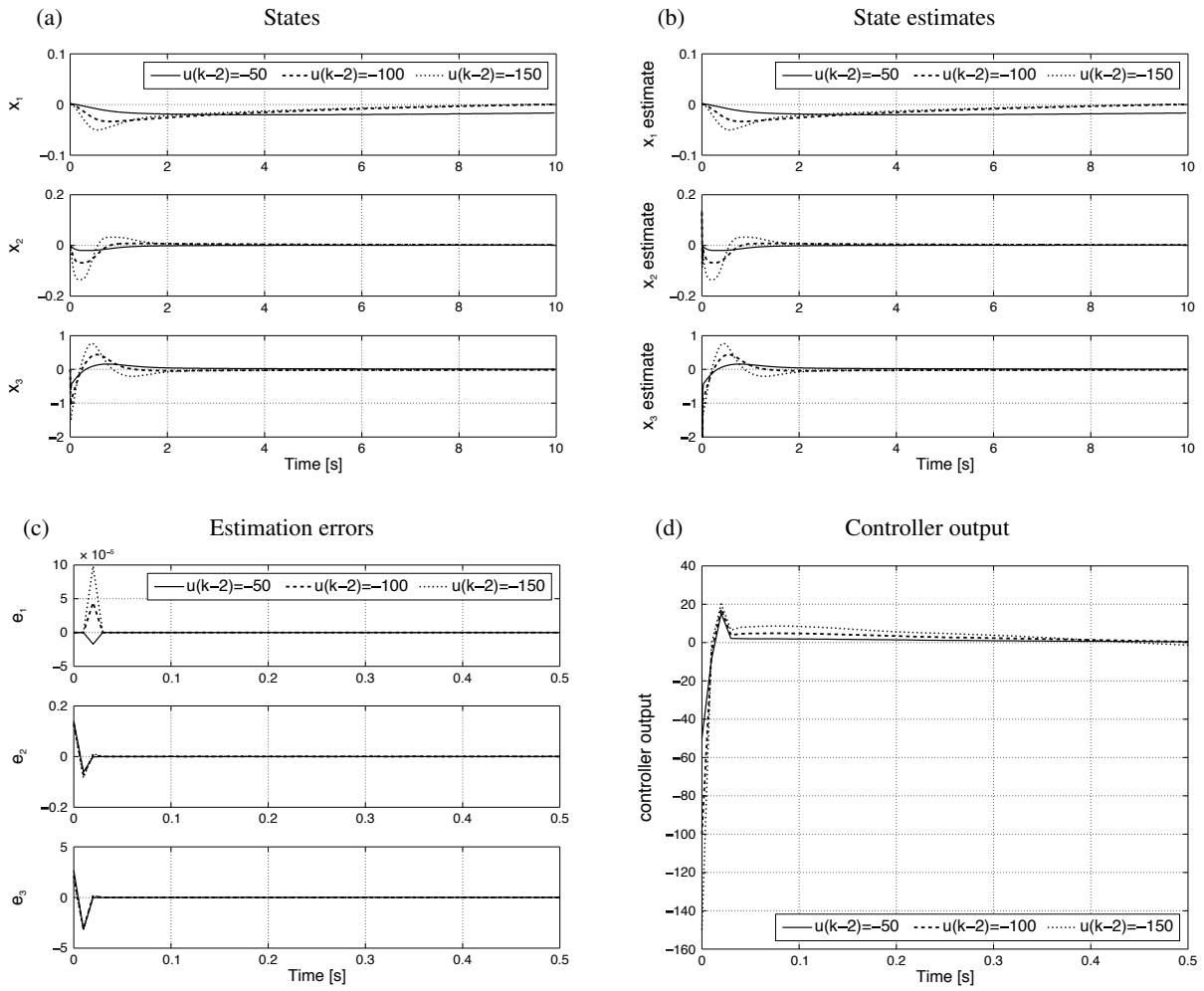

Fig. 4. Responses of the observer-based closed-loop system (3) and (8a) for different initial values of the controller output.

Figure 5 presents the Newton observer-based feedback responses to different controllers (8a), (8b), and (8c). The system trajectories and their estimates are compared for each controller. Also in this time, the estimate of the state vector $x = [x_1\ x_2\ x_3]^{\mathsf{T}}$, in particular the magnetic flux, demonstrates satisfactory performance. Notice that the closed-loop system stability and performance depend on the controller structure (see [16] for details). The estimation errors $e_i = (\hat{x}_i - x_i)$ for $i = 1,2,3$ in the simulations converge to zero in time.

For the simulation results from Figs 2–5, we assumed $\varepsilon = 0$, i.e. the AMB system was reduced to the zero-bias case. Next simulations in Fig. 6 present the nonzero-bias flux AMB system responses with fixed $\varepsilon = 2\Phi_0/\Phi_{\text{sat}}$, where the influence of the bias flux Φ_0 on the AMB system responses is evaluated, whereas $\Phi_{\text{sat}} = 0.0022$ Wb. Comparison of the low-bias ($0 < \varepsilon \ll 1$) and zero-bias ($\varepsilon = 0$) AMB observer-based feedback responses to the initial conditions is presented in Fig. 6. The obtained results for the flux estimation are similar, which confirms the robustness of the Newton observer.

The simulation results demonstrate that the performance of the Newton observer and observer-based closed-loop system under the three control laws (8) is good in spite of the control voltage saturation and the AMB nonlinearities. Both the observer-based feedback-controlled trajectories and the state feedback-controlled trajectories without observer as well as control signals meet the desired performance. The settling time is below 10 s for all simulations while the absolute value of the control voltage does not exceed 150 V.

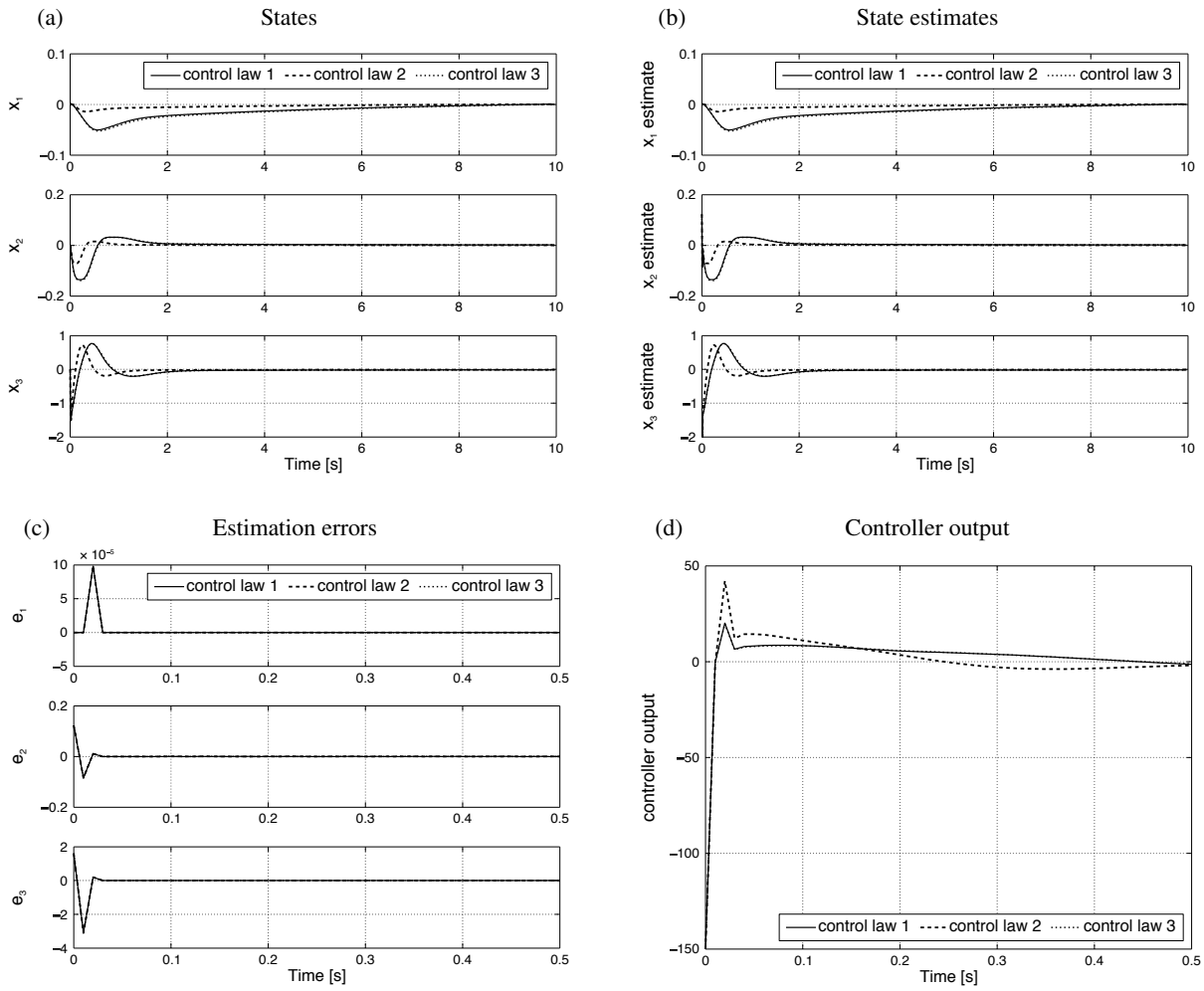

Fig. 5. Observer-based feedback responses to the different control laws (8a), (8b), and (8c).

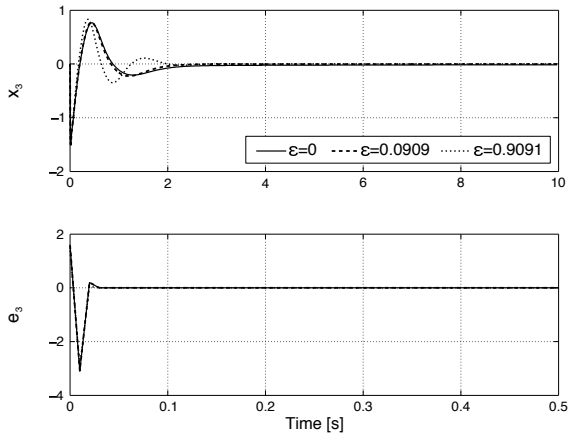

Fig. 6. Observer-based feedback responses to the initial conditions with the zero-bias flux $\Phi_0 = 0$ and the low-bias flux $\Phi_0 = 100, 1000\ \mu$Wb and with the control law (8a).

5. CONCLUSIONS

The Newton observer was adapted for magnetic flux estimation in a flux-controlled nonlinear AMB system (with singularity of the flux function), based on its exact discrete-time model. The effectiveness of the observer was verified via the simulations when it was combined with the nonlinear controllers for rotor mass stabilization, suggested in [17]. The simulations showed global asymptotic stability and good performance (convergence) of the Newton observer-based closed-loop system. One of the topics for future research is extension of the results of this paper for physical 5-DOF AMB system from [15], combined with the Lyapunov Control Function based controllers.

ACKNOWLEDGEMENTS

The work of A. Mystkowski is supported with Statutory Work of the Department of Automatic Control and Robotics, Faculty of Mechanical Engineering, Białystok University of Technology (No. S/WM/1/2016). The work of Ü. Kotta and V. Kaparin is supported by the Estonian Research Council, personal research funding grant PUT481. The publication costs of this article were covered by the Estonian Academy of Sciences.

REFERENCES

1. Arcak, M. and Kokotović, P. Observer-based control of systems with slope-restricted nonlinearities. *IEEE Trans. Autom. Control*, 2001, **46**, 1146–1150.
2. Baloh, M., Tao, G., and Allaire, P. Modeling and control of a magnetic bearing actuated beam. In *Proceedings of the 2000 American Control Conference, Chicago, IL, USA* (Zhu, J., ed.), Vol. 3. IEEE, 2000, 1602–1606.
3. Baranowski, J. and Tutaj, A. Continuous state estimation in water tank system. In *Computer Methods and Systems, VI Konferencja Metody i Systemy Komputerowe, Kraków, Poland* (Tadeusiewicz, R., Ligeza, A., and Szymkat, M., eds). ONT, 2007, 373–378.
4. Bıyık, E. and Arcak, M. A hybrid redesign of Newton observers in the absence of an exact discrete-time model. *Syst. Control Lett.*, 2006, **55**, 429–436.
5. Chen, S.-L. and Hsiao, Y.-H. Nonlinear high-gain observer for a three-pole active magnetic bearing system. In *The 8th Asian Control Conference, Kaohsiung, Taiwan*. IEEE, 2011, 155–159.
6. Farkhatdinov, I., Hayward, V., and Berthoz, A. On the benefits of head stabilization with a view to control balance and locomotion in humanoids. In *The 11th IEEE-RAS International Conference on Humanoid Robots, Bled, Slovenia*. IEEE, 2011, 147–152.
7. Grossman, W. D. *Observers for Discrete-time Nonlinear Systems*. PhD thesis, New Jersey Institute of Technology, 1999.
8. Kotta, Ü. Discrete-time models of a nonlinear continuous-time system. *Proc. Estonian Acad. Sci. Phys. Math.*, 1994, **43**, 64–78.
9. Lin, Z. and Knospe, C. A saturated high gain control for a benchmark experiment. In *The American Control Conference, Chicago, IL, USA* (Zhu, J., ed.), Vol. 4. IEEE, 2000, 2644–2648.
10. Maslen, E. *Magnetic Bearings*. Graduate Seminar Notes, Department of Mechanical and Aerospace Engineering, University of Virginia, 2000.
11. Mizuno, T., Araki, K., and Bleuler, H. Stability analysis of self-sensing magnetic bearing controllers. *IEEE Trans. Control Syst. Technol.*, 1996, **4**, 572–579.
12. Monaco, S. and Normand-Cyrot, D. On the sampling of a linear analytic control system. In *The 24th IEEE Conference on Decision and Control, Fort Lauderdale, FL, USA*. IEEE, 1985, 1457–1462.
13. Moraal, P. E. *Nonlinear Observer Design: Theory and Applications to Automotive Control*. PhD thesis, University of Michigan, 1994.
14. Moraal, P. E. and Grizzle, J. W. Observer design for nonlinear systems with discrete-time measurements. *IEEE Trans. Autom. Control*, 1995, **40**, 395–404.
15. Mystkowski, A. Sensitivity and stability analysis of mu-synthesis AMB flexible rotor. *Solid State Phenom.*, 2010, **164**, 313–318.
16. Mystkowski, A. and Pawluszewicz, E. Remarks on some robust nonlinear observer and state-feedback zero-bias control of AMB. In *The 16th International Carpathian Control Conference, Szilvásvárad, Hungary* (Petráš, I., Podlubny, I., Kačur, J., and Vásárhelyi, J., eds). IEEE, 2015, 328–333.
17. Mystkowski, A., Pawluszewicz, E., and Dragašius, E. Robust nonlinear position-flux zero-bias control for uncertain AMB system. *Int. J. Control*, 2015, **88**, 1619–1629.

18. Noshadi, A., Shi, J., Lee, W. S., Shi, P., and Kalam, A. Robust control of an active magnetic bearing system using H_∞ and disturbance observer-based control. *J. Vib. Control*, 2017, **23**, 1857–1870.
19. Torres, M., Sira-Ramirez, H., and Escobar, G. Sliding mode nonlinear control of magnetic bearings. In *Proceedings of the 1999 IEEE International Conference on Control Applications, Kohala Coast, HI, USA*, Vol. 1. IEEE, 1999, 743–748.
20. Tsiotras, P. and Arcak, M. Low-bias control of AMB subject to voltage saturation: state-feedback and observer designs. *IEEE Trans. Control Syst. Technol.*, 2005, **13**, 262–273.
21. Tsiotras, P. and Velenis, E. Low-bias control of AMB's subject to saturation constraints. In *Proceedings of the 2000 IEEE International Conference on Control Applications, Anchorage, AK, USA*. IEEE, 2000, 138–143.
22. Tsiotras, P., Wilson, B., and Bartlett, R. Control of zero-bias magnetic bearings using control Lyapunov functions. In *Proceedings of he 39th IEEE Conference on Decision and Control, Sydney, Australia*, Vol. 4. IEEE, 2000, 4048–4053.
23. Tsiotras, P. and Wilson, B. C. Zero- and low-bias control designs for active magnetic bearings. *IEEE Trans. Control Syst. Technol.*, 2003, **11**, 889–904.
24. Vischer, D. and Bleuler, H. Self-sensing active magnetic levitation. *IEEE Trans. Magn.*, 1993, **29**, 1276–1281.

Newtoni olekutaastaja mittelineaarse aktiivse magnetlaagri jaoks

Arkadiusz Mystkowski, Ülle Kotta ja Vadim Kaparin

On kirjeldatud Newtoni olekutaastaja kohandamist magnetvoo hindamiseks mittelineaarse aktiivse magnetlaagersüsteemi tagasisidega juhtimisel. Newtoni olekutaastaja konstrueeriti magnetlaagersüsteemi täpse diskreetaja mudeli jaoks. Tulemus esitati detailse ja lihtsa rakendusalgoritmina. Newtoni olekutaastajat kombineeriti kolme kontrolleriga, mille efektiivsust verifitseeriti Matlabi tarkvara abil tehtud simulatsioonide põhjal.